Green organic conversion with H₂O₂: challenges and opportunities

Xiaoming Xu[1,2], Yuanming Zhang[1,2], Yong Chen[3], Changhao Liu[1,2], Yang Li[1,2], Zhonghua Li[1,2], Zhetong Yang[1,2], Zhaosheng Li[1,2]* and Zhigang Zou[1,2]

Hydrogen peroxide (H₂O₂), as a green oxidant, plays an important role in organic conversion reactions, such as cyclohexanone ammoximation and olefin oxidation. However, the production of H₂O₂ relies on the anthraquinone process, which is costly, complex, and typically done on clustered production. Furthermore, H₂O₂ is prone to decomposition or the generation of ineffective byproducts and unfavorable reactive groups, leading to low efficiency and waste of resources. Achieving the widespread application of H₂O₂ in green organic conversion reactions requires efficient utilization and low-cost on-site production of H₂O₂. Effective activation of H₂O₂ is the key to realizing efficient utilization of H₂O₂, which has been widely recognized. In addition, some emerging methods of on-site production of H₂O₂ are convenient and low-cost. These methods may gradually overcome the shortcomings of traditional methods in the future. In this review, we introduce common organic conversion reactions with H₂O₂, summarize the challenges of H₂O₂ activation, and review the progress on electrochemical, photoelectrochemical or photochemical H₂O₂ production. We also discuss the vision of organic conversion reactions via in-situ-generated H₂O₂.
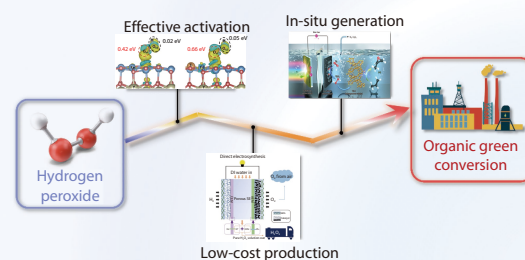
In modern chemical industry, the production of chemicals involves a variety of chemical reactions, and more than 50% of chemicals require oxidation reactions.[1–3] H₂O₂, as a green and low-cost oxidant, has a wide range of applications in chemical synthesis, including driving the cyclohexanone ammoximation, the epoxidation of olefins, the oxidation of alcohols, and the conversion of olefins to aldehydes and so on.[4, 5, 67, 68] The H₂O₂-mediated reaction methods show the advantages of environmental friendliness and process simplification. However, in these reactions, the H₂O₂ is mostly produced by the anthraquinone process,[6] which suffers from low hydrogenation efficiency, complex process, high consumption, low single-unit yield, and limitations of clustered production, making the widespread application of H₂O₂ extremely difficult and expensive. Furthermore, the utilization efficiency of H₂O₂ is limited by its concentration dependence and ineffective decomposition and evolution, resulting in energy waste and low reaction efficiency. Therefore, achieving low-cost on-site production and effective utilization of H₂O₂ has become the focus topic.

Activation of H₂O₂ molecules is the core of efficient utilization of H₂O₂. In most reactions, H₂O₂ itself or activated free radicals and non-radical reactive species act as oxidants, driving the oxidation reaction of organic molecules.[7, 8] The production of reactive species requires an activation process involving electron transfer and chemical bond breaking.[9] This process determines the production rate and type of active species, which not only affects the efficiency of organic conversion reaction, but also decides the selectivity of products. Therefore, extensive researches on effective activation strategies of H₂O₂ molecules are extremely necessary. Recently, many H₂O₂ production processes (electrochemical, photoelectrochemical or photochemical methods) can be achieved through oxygen reduction reaction (ORR) or water oxidation reaction (WOR) in a simpler reaction system using re-generated light or electric energy. These methods have attracted wide attention due to their advantages of simple process, single product and low cost, and created the possibility of replacing anthraquinone method to produce H₂O₂ on site with low energy consumption.[10, 11] Furthermore, in-situ generation of H₂O₂ has been proposed, directly participating in the conversion of organic molecules,[12, 13] avoiding the complex purification and other multi-step process of H₂O₂, and

1 *Collaborative Innovation Center of Advanced Microstructures, National Laboratory of Solid State Microstructures, College of Engineering and Applied Sciences, Nanjing University, Nanjing 210093, China*

2 *Jiangsu Key Laboratory of Nano Technology, Nanjing University, Nanjing 210093, China*

3 *School of New Energy, Nanjing University of Science and Technology, Jiangyin 214400, China*

* Corresponding author, E-mail: zsli@nju.edu.cn

achieving more direct and efficient application of H_2O_2. These studies and strategies provide creative development ideas for the application of H_2O_2 in green organic conversion, but they also face many significant challenges and opportunities.

In this review, we will discuss the organic conversion reactions with H_2O_2, the challenges and opportunities of H_2O_2 activation studies, new advances in the efficient H_2O_2 production, and the prospects of organic conversion reactions via in-situ-generated H_2O_2.

H_2O_2-mediated organic conversion reaction

Cyclohexanone ammoximation

Cyclohexanone ammoximation (Figure 1a) is a crucial step in the production of caprolactam.[5] Caprolactam is mainly used to produce polyamide chips (nylon-6 chips) by polymerization, which can be further processed into nylon fibers, engineering plastics, plastic films, and other products. In the 1980s, Marko et al.[14] developed a cyclohexanone ammoxim-
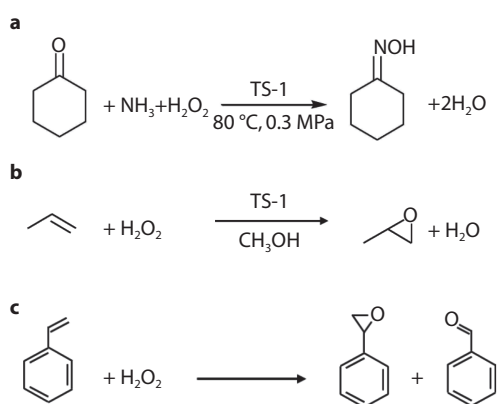
ation process using H_2O_2 as an oxidant (TS zeolite as a catalyst and NH_3 as a nitrogen source) to achieve high conversion and selectivity under mild reaction conditions. The conversion rate of cyclohexanone was above 99.0%, and the selectivity of cyclohexanone oxime was higher than 98.2%.[5] This has led to extensive attention and research on the H_2O_2-mediated organic conversion process.[15]

Oxidation of alkenes

The hydrogen peroxide propylene oxide (HPPO) is considered a new green process for producing propylene oxide, which is an environmentally friendly and clean production system.[4] This process uses titanium silicalite-1 (TS-1) as a catalyst to promote the epoxidation reaction of propylene with H_2O_2, resulting in the formation of water and propylene oxide (Figure 1b).[16] Since 2008, the HPPO process has demonstrated high efficiency, with an annual production capacity of up to 300,000 tons of propylene oxide and a selectivity of 95%.[17] This has also led to extensive attention on the H_2O_2-mediated oxidation of alkenes.

Fig. 1 **a** Reactions involved in cyclohexanone ammoximation methods.[5] Copyright 2021, Elsevier. **b** Industrial processes for propylene oxide production through the hydrogen peroxide propylene oxide (HPPO) process. **c** A plausible reaction pathway for the epoxidation of styrene. **d** Production of adipic acid with H_2O_2.[23] Copyright 2006, John Wiley and Sons. **e** Selective oxidation of (E)-cinnamyl alcohol with H_2O_2 using continuous flow reactors.[28] Copyright 2021, Royal Society of Chemistry.

Oxidation of styrene

Styrene oxide is an important organic molecule widely used as an epoxy resin diluent, UV absorber, fragrance enhancer.[18] In traditional processes, styrene oxide is produced by dehydrochlorination of styrene chlorohydrin under strong alkaline or acidic conditions.[19] However, the use of harmful chemicals generates a large amount of corrosive and hazardous waste, causing environmental pollution. Therefore, the use of transition metal catalysts with hydrogen peroxide as an oxidizing medium has gradually replaced the traditional synthetic route for producing styrene oxide (Figure 1c).[20] In the H_2O_2-mediated epoxidation process, the properties of catalysts and related reaction parameters determine whether it evolves into a styrene oxide or benzaldehyde through superoxide or hydroxyl radicals.[8, 20-22]
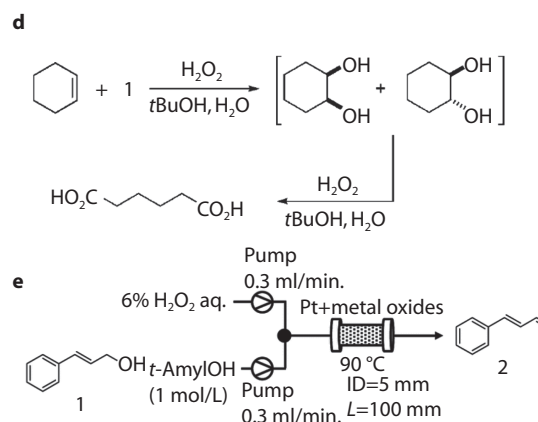
Preparation of dicarboxylic acid by olefin cleavage

Dicarboxylic acid is an important raw material for the production of polyester and polyamide, and has been widely used in various fields such as fiber, lubricant, pharmaceutical, pesticide, cosmetic, and plasticizer manufacturing.[17, 23, 24]

The H_2O_2-mediated C=C bond cleavage reaction (Figure 1d) generates various oxygen-containing compounds depending on the functional groups (ketones, aldehydes, and carboxylic acids) carried by the double bond and the experimental conditions. In this type of reaction, transition metal catalysts receive more attention mainly because they typically have unsaturated electronic structures that are more easily coordinated with H_2O_2 molecules, forming highly active complexes to increase the activation efficiency of C–C double bonds.[17, 23] Timofeeva et al. obtained yields of 18% and 33% for adipic acid by H_2O_2 oxidation cracking of cyclohexene using transition metal silicate Ti-MMM-2 and Ce-SBA-15, respectively.[24]

Oxidation of alcohol

Selective oxidation of alcohol to their corresponding aldehydes or esters is one of the most important conversions in the synthesis of various fine chemicals.[25, 26, 69, 70] Although H_2O_2 is a clean oxidant, it easily leads to the overoxidation of alcohols to form acids.[27] Therefore, appropriate catalysts are required to regulate the reaction process. Kon et al. used a

catalyst consisting of Pt dispersed on SiO_2 to achieve a conversion rate of more than 95% of (E)-cinnamyl alcohol to (E)-cinnamaldehyde (Figure 1e).[28] Wang et al. demonstrated that a single-atom cobalt compound supported by a pure inorganic ligand, $(NH_4)_3[CoMo_6O_{18}(OH)_6]$ (abbreviated as $CoMo_6$), can serve as a heterogeneous catalyst. Under mild conditions with 30% H_2O_2, the oxidation cross-esterification of various alcohols (aromatic and aliphatic) can be achieved.[29]

Effective activation of H_2O_2 molecules

In most organic reactions where H_2O_2 serves as the oxidant, the true active species may be H_2O_2, •OH, •O_2^-, or $^1O_2$. [9, 20, 30]

The activation of H_2O_2 involves various configuration adsorption, bond stretching, and electron transfer processes. Intermediate species often play a key role in these processes. They may be influenced by the local structure and charge distribution of active centers, altering the rate of H_2O_2 activation, regulating the activation pathway, and controlling product selectivity.[9] In addition, the interaction between active oxygen species and organic molecules determines the reaction rate and product selectivity. For example, in the oxidation of styrene, •O_2^- radicals induce the formation of styrene oxide, while •OH radicals induce the formation of benzaldehyde (Figure 2a).[8] And the oxidation of benzyl alcohol is more selective to benzaldehyde products under the induction of •O_2^-
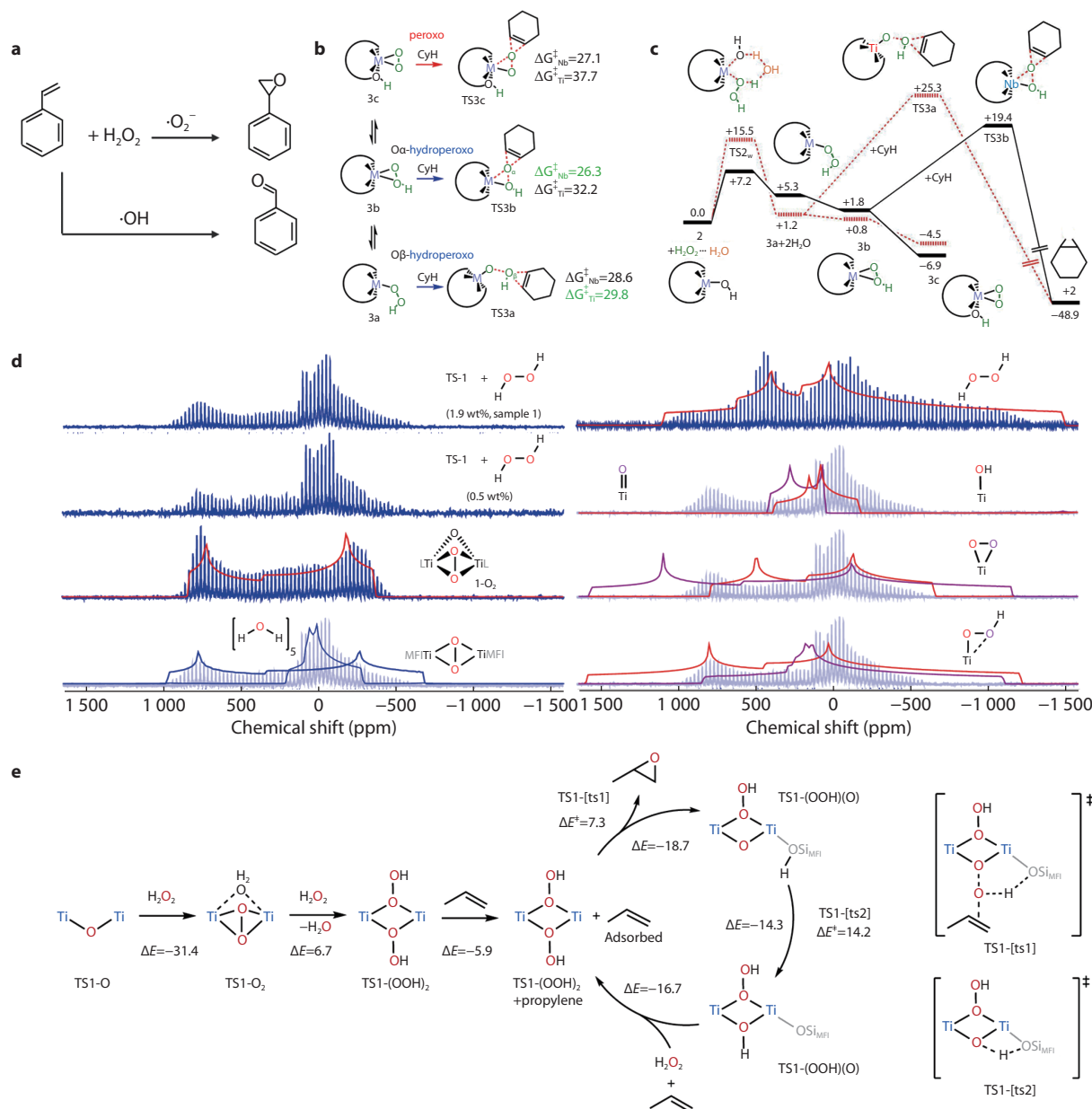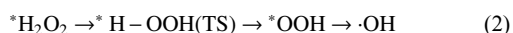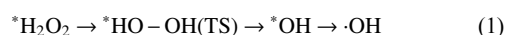

Fig. 2 **a** Reaction paths of styrene under different oxygen radicals. **b** Possible pathways for oxygen transfer to CyH from peroxo and hydroperoxo species in transition-metal-substituted polyoxometalates. **c** Calculated potential free-energy profile (kcal mol⁻¹) for cyclohexene epoxidation with H_2O_2.[32] Copyright 2019, American Chemical Society. **d** Experimental and calculated solid-state ^{17}O NMR spectra. **e** Calculated energy surface of propylene epoxidation at a dinuclear Ti site (electronic energies are given in kcal mol⁻¹).[7] Copyright 2020, Springer Nature.

radical or $^1O_2$, while the selectivity for benzoic acid is more prominent under the induction of •OH radical. Therefore, to effectively activate H_2O_2, it is necessary not only to focus on its activation rate but also to control its activation products. Identification of catalytic active centers and visual detection and regulation of activation path will determine the utilization efficiency of H_2O_2.

Identification of catalytic active centers

In the reaction systems of classic catalysts such as Lindqvist-structured tungstate and TS-1, in which H_2O_2 directly participates in the reaction as oxidizing species, the understanding of the active sites that truly activate H_2O_2 is still limited.[7, 31, 32] Recently, Carbo's group discovered that M-substituted tungstate (M: Ti, Nb, Zr, etc.) with Lindqvist structure formed new active metal sites with M metal, showing higher catalytic activity and selectivity in the epoxidation of cyclohexene (Figure 2b).[31, 32] MW_5 or its hydrolysate "MOH" interacted with H_2O_2 to produce protonated peroxide species "MOOH" (Figure 2c). Then, the electrophilic oxygen atom transfered from "MOOH" to the C-C bond, generating epoxy compounds and "MOH". Moreover, it has long been believed that the catalytic performance of TS-1 is attributed to isolated Ti (IV) sites within the zeolite framework, but this has not been confirmed. Combining spectroscopy and microscopy, Copéret's group found that bridging peroxo groups were formed on the binuclear Ti site after contact with $H_2^{17}O_2$ (Figures 2d).[7] In addition, the synergistic effect between the two Ti atoms enabled the epoxidation of propylene to proceed through a low-energy reaction pathway with a key oxygen transfer transition state similar to the peracid epoxidation of olefins. This confirms that the high efficiency of TS-1 in the catalytic epoxidation of propylene with H_2O_2 is due to the binuclear Ti atoms, rather than isolated Ti atoms, obtaining a novel interpretation of the real catalytic active center (Figure 2e).
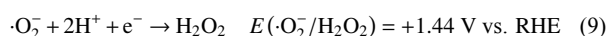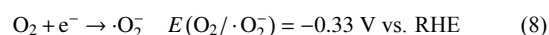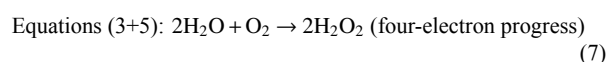
$$^*H_2O_2 \rightarrow {}^*HO-OH(TS) \rightarrow {}^*OH \rightarrow \cdot OH \quad (1)$$

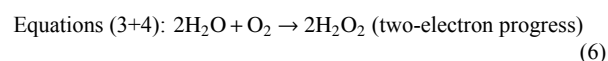$$^*H_2O_2 \rightarrow {}^*H-OOH(TS) \rightarrow {}^*OOH \rightarrow \cdot OH \quad (2)$$
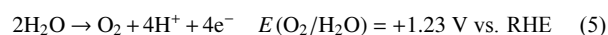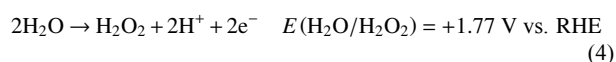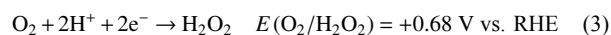
Visual detection and regulation of activation path

Due to the extremely short lifetime of intermediate species and the difficulty to track and detect, the processes of H_2O_2 activation to produce •OH, •O_2^-, and $^1O_2$ are largely speculative. Among them, there is a controversy over the formation pathway of the •OH radical, which could occur through either HO-OH (TS) (Equation.1) or H-OOH (TS) (Equation.2) mediation.[9, 33, 34] Traditionally, it was believed that H_2O_2 was activated through the HO-OH (TS) pathway.[33] Recently, our group utilized in situ shell-isolated nanoparticle-enhanced Raman spectroscopy (SHINERS) technology, combined with isotope labeling and density functional theory calculations (Figures 3a, 3b and 3c), to demonstrate the essential formation of *OOH and *OH species in H_2O_2 activation progress on the surface of $YFeO_3$.[9] H_2O_2 formed a single oxygen adsorption configuration on the Fe site, which led to the cleavage of H-O bond to form *OOH (Figures 3d and 3e). Subsequently, *OH species were formed through electron transfer and O-O bond cleavage (Figures 3f and 3g). We confirmed the existence of the H-OOH (TS) mediated pathway to distinguish the controversy and proposed to accelerate the activation process of

H_2O_2 by regulating the surface charge (Figure 3h) and local structure (Figure 3i) of $YFeO_3$ catalysts. Therefore, visualization of activation process can provide guidance for the design of efficient catalysts. H_2O_2, •OH, •O_2^-, and $^1O_2$ have different oxidation abilities, which means that they can induce different products in organic reactions. However, achieving controllable selection of H_2O_2 activation products (•OH, •O_2^-, or $^1O_2$) is a key challenge. Zhang's group achieved effective control of •OH and •O_2^- by loading single-atom layer Cu_5 nanoclusters onto the surface of FeS_2.[35] Pan's group realized controllable selection of •OH and $^1O_2$ by using a C nanotube-confined Fe_2O_3 system.[36] Xing's group constructed a $CoFe_2O_4/MoS_2$ heterostructure, which decomposed H_2O_2 to generate •OH with limited migration distance, leading to the formation of $^1O_2$.[37]

Low-cost on-site production of H_2O_2

The production process and equipment for anthraquinone synthesis are complex and more suitable for large-scale production.[10] This process may generate a large carbon footprint and organic waste, and centralized H_2O_2 production requires transportation and storage of unstable and hazardous bulk H_2O_2 solutions. The electrochemical, photoelectrochemical or photochemical methods, using renewable electric or solar energy as inputs, provide an economic and green pathway for on-site H_2O_2 production.[38-40]

$$O_2 + 2H^+ + 2e^- \rightarrow H_2O_2 \quad E(O_2/H_2O_2) = +0.68 \text{ V vs. RHE} \quad (3)$$

$$2H_2O \rightarrow H_2O_2 + 2H^+ + 2e^- \quad E(H_2O/H_2O_2) = +1.77 \text{ V vs. RHE} \quad (4)$$

$$2H_2O \rightarrow O_2 + 4H^+ + 4e^- \quad E(O_2/H_2O) = +1.23 \text{ V vs. RHE} \quad (5)$$

Equations (3+4): $2H_2O + O_2 \rightarrow 2H_2O_2$ (two-electron progress) (6)

Equations (3+5): $2H_2O + O_2 \rightarrow 2H_2O_2$ (four-electron progress) (7)

$$O_2 + e^- \rightarrow \cdot O_2^- \quad E(O_2/\cdot O_2^-) = -0.33 \text{ V vs. RHE} \quad (8)$$

$$\cdot O_2^- + 2H^+ + e^- \rightarrow H_2O_2 \quad E(\cdot O_2^-/H_2O_2) = +1.44 \text{ V vs. RHE} \quad (9)$$

Electrochemical and photoelectrochemical H_2O_2 production

The reaction system for electrochemical and photoelectrochemical H_2O_2 production is based on either the two-electron process (Equations 3,4 and 6) or the four-electron process (Equations 3, 5 and 7), mainly via the cathodic ORR or the anodic WOR in Figures 4a and 4b.[38, 41] The four-electron process requires twice the amount of photons/current to produce the same amount of H_2O_2 as in the two-electron process.[38] Recent studies by Hu et al. showed that, in the absence of anodic water oxidation for H_2O_2 production, only H_2O_2 produced via cathodic ORR can serve as a reducing agent and be consumed in the anodic oxygen evolution reaction (OER).[11] Therefore, the two-electron process may be superior to the four-electron process, arousing increasing interest in finding selective 2e$^-$-ORR catalysts. The selectivity for H_2O_2 production via ORR (Equation 4) is related to the ability of the intermediate OOH* species to adsorb on the catalyst
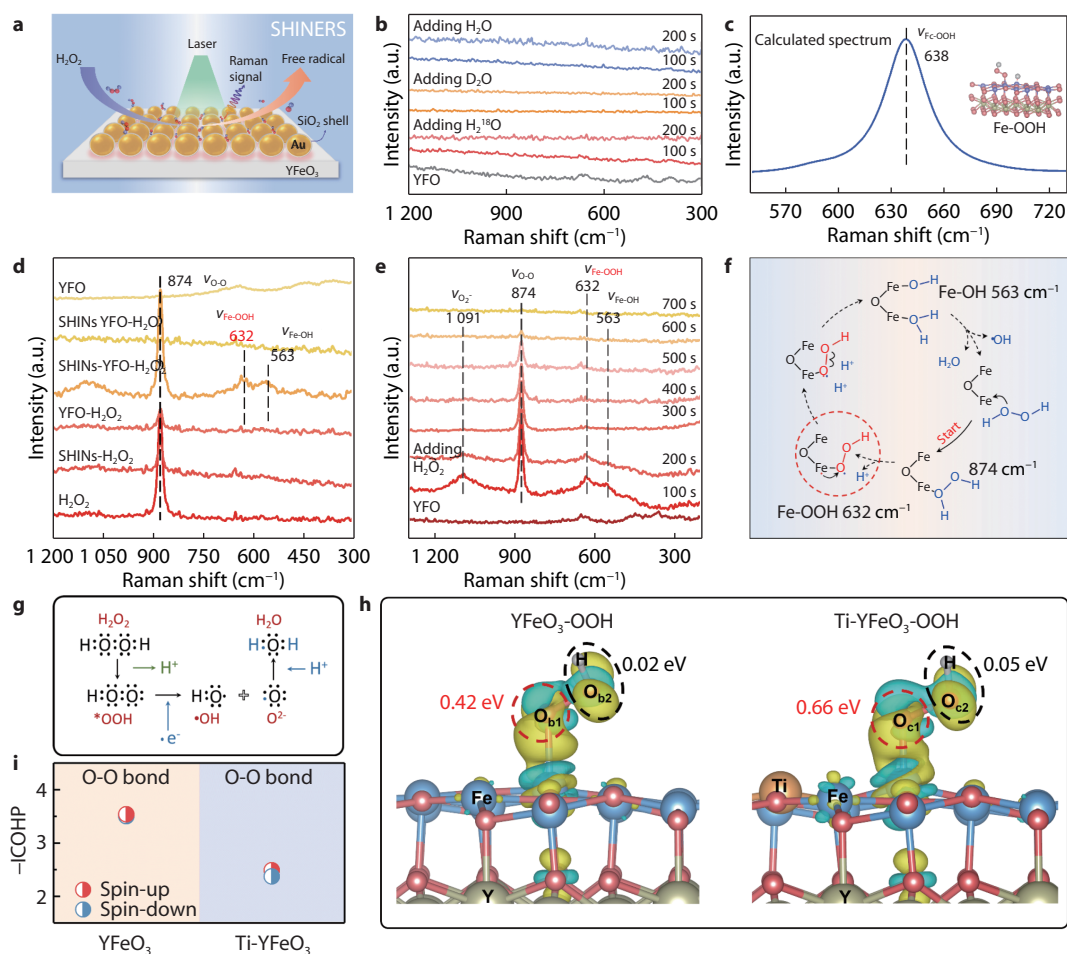
Fig. 3 **a** Schematic of shell-isolated nanoparticle-enhanced Raman spectroscopy (SHINERS) detection process. **b** SHINERS spectra of isotope labelling. **c** The correlated Raman frequencies of the Fe-O stretching vibration for Fe-OOH species (grey: H, red: O, blue: Fe and yellow: Y). **d** SHINERS spectra in different systems. **e** SHINERS spectra in the decomposition process of H_2O_2 as a function of time. **f** The possible mechanism for the activation process of H_2O_2. **g** Electron transfer process in the formation of •OH by H_2O_2 activation. **h** The different charge densities of *OOH adsorbed on $YFeO_3$ (left) and Ti-$YFeO_3$ (right). **i** The corresponding integral crystal orbital Hamilton populations (ICOHP) in $YFeO_3$-OOH and Ti-$YFeO_3$-OOH.[9] Copyright 2022, National Academy of Science.

surface, and this issue has received broader attention.[42] In the 1930s, Berl first reported the small-scale on-site H_2O_2 production route via the electrochemical 2e⁻-ORR.[43] Until to 2019, Wang's group reported the design of a porous solid electrolyte that delivered independent H_2 and O_2 flows to the electrode catalysts coated with gas diffusion layers (GDLs) for the H_2 oxidation reaction (HOR) and 2e⁻-ORR processes (Figure 4c), respectively.[44] The generated H⁺ and HO_2⁻ ions crossed from the positive and negative electrodes in the intermediate layer, and the catalyst activity and selectivity can be maintained for 100 hours (Figure 4d). The flowing deionized water can dissolve pure H_2O_2 products, yielding a pure H_2O_2 solution with a concentration of up to 20 wt%. This breakthrough has attracted widespread attention in the academic community. Wu et al. discovered that cationic surfactants can effectively serve as in situ kinetic promoters for the oxygen-peroxide reaction on carbon black electrodes (Figure 4e). In alkaline media, within a window of 0.8 V, the peroxide yield reached over 90% (up to 95.2%), achieving the best H_2O_2 electrocatalyst at that time (Figures 4f).[45] Close to

(~90%) selectivity can also be achieved by photoelectrochemical methods. Recently, Zhang et al. thermally annealed metal-doped hematite mesocrystals at relatively low temperatures and in air, eliminating grain boundaries and obtaining many oxygen vacancies in the bulk. This resulted in the effective separation of the dopant (~90%) on the outer surface, forming an oxide coating. High activity (~0.8 μmol min⁻¹ cm⁻²) and selectivity (~90%) for photoelectrochemical H_2O_2 production were achieved by hematite mesocrastic photoanodes containing Sn and Ti dopant oxide coatings.[71] To date, many types of efficient catalysts and reaction devices have been researched and designed, making electrochemical and photoelectrochemical H_2O_2 production a possible route for industrial applications.[46]

Photochemical H_2O_2 production

Photochemistry is a promising approach for producing H_2O_2 through the input of light energy, which is more environmentally friendly and sustainable.[39] However, this process is faced with challenges such as low reaction efficiency. The photocatalytic system relies mainly on two electron pro-
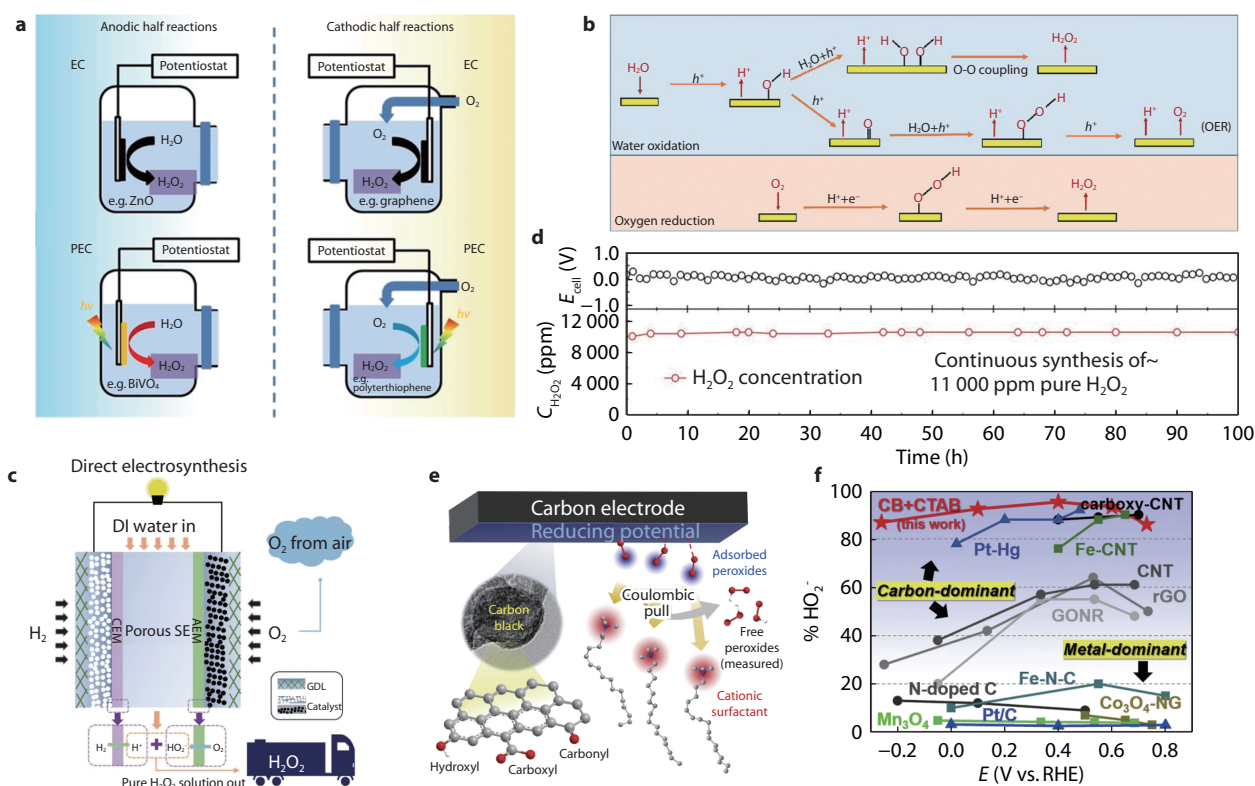
Fig. 4   a Schematic illustration of H_2O_2 production in a half-reaction achieved by water oxidation and oxygen reduction.[38] Copyright 2020, John Wiley and Sons. **b** Schematic illustration of ORR and WOR pathways.[40] Copyright 2022, Elsevier. **c** Electrochemical of H_2O_2 production using pure H_2 and O_2 streams separately introduced to the anode and cathode, respectively. **d** Stability tests for continuous generation of pure H_2O_2 solutions with concentrations >10,000 ppm. [44] Copyright 2019, American Association for the Advancement of Science. **e** In situ selectivity modulation by surface-acting cations at the carbon surface. **f** Comparisons of peroxide selectivity and potential window width among reported electrocatalyst systems.[45] Copyright 2020, Elsevier.

cesses. Photo-generated electrons participate directly in the ORR via proton-coupled electron transfer, while photo-generated holes react with electron donors to provide protons. The two-electron process occurs mainly through direct two-electron mechanisms (Equation 3) or intermediate mechanisms involving $\cdot O_2^-$ (Equations 8 and 9).[47] Direct two-electron ORR pathways (+ 0.68 V vs. normal hydrogen electrode) are thermodynamically more favorable than indirect double-electron pathways (− 0.33 V vs. normal hydrogen electrode) as shown in Figure 5a. However, the indirect ORR process is kinetically favored because only one electron is required in each step (Figure 5b). This also leads to lower H_2O_2 formation efficiency in the indirect ORR process mechanism. The choice of photocatalysts is critical for addressing these challenges. Recently, new types of coordination compounds with two- or three-dimensional structures, such as metal-organic frameworks and covalent organic frameworks,[47–49] have been extensively studied due to their excellent photocatalytic activity. Zhu's group reported a self-assembled tetra (4-carboxyphenyl) porphyrin (SA-TCPP) supramolecular photocatalyst can produce H_2O_2 through reactions at different active sites (Figures 5c).[48] As shown in Figure 5d, the quantum efficiency of H_2O_2 production from H_2O and O_2 under 420 nm is 9.420%, while that under 940 nm is 1.940%. This catalyst achieves an extremely high solar-to-chemical conversion efficiency of 1.2% at 328 K under simulated solar light irradiation.

Organic conversions via in-situ-generated H_2O_2

The low stability of H_2O_2 and its tendency to rapidly decompose at relatively mild temperatures require the use of stabilizers such as acetic acid and phosphoric acid.[12, 50] The reactor corrosion, catalytic instability, and the need to remove stabilizers from the product stream further complicate the matters. In-situ-generated H_2O_2 can participate directly in organic conversion reactions, avoiding the aforementioned issues and greatly enhancing its utility.[51, 52] In this system, H_2O_2 tends to be generated directly from H_2/O_2, with highly effective Pd-based catalysts.[53] Pd-based catalysts supported on porous carriers are valuable industrial catalysts, such as Pd nanoparticles-supported TS-1 used for epoxidation of propylene.[54] Au-Pd/TS-1 also exhibits high activity in selective oxidation of benzyl alcohol and cyclohexanone ammoximation via in-situ-generated H_2O_2.[55, 56]

However, in the actual reaction system, the mismatch of the optimal conditions between H_2O_2 generation and organic conversion is a key challenge. For example, direct generation of H_2O_2 is supported by acidic conditions and low ambient temperature, while the ammoximation of cyclohexanone is associated with high temperature (80-140 ℃) and the use
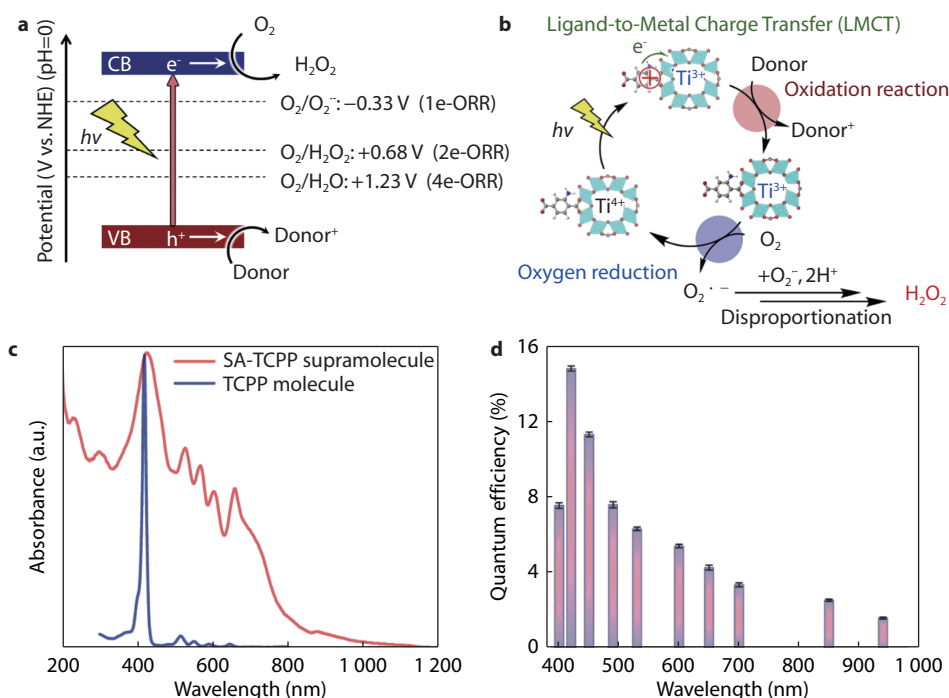
Fig. 5 **a** Energy diagram for photocatalytic H_2O_2 production via oxygen reduction. **b** Proposed reaction mechanism for photocatalytic H_2O_2 production.[47] Copyright 2022, Elsevier. **c** UV-vis-NIR DRS of SA-TCPP supramolecular assembly and UV–vis absorption spectrum of TCPP molecules. The strongest peak of SA-TCPP and TCPP molecules is located approximately at 415-430 nm. In contrast to TCPP molecules, the energy band absorption of SA-TCPP nanosheets extends up to 1,100 nm. **d** Quantum efficiency on SA-TCPP supramolecular photocatalysts with different bandpass filters.[48] Copyright 2023, Springer Nature.

of ammonia.[57] In 2022, Lewis et al. used gold-palladium (AuPd) alloy nanoparticles-supported TS-1 catalyst to achieve cyclohexanone ammoximation reaction via in-situ-generated H_2O_2 (Figure 6a), obtaining high yield cyclohexanone oxime with the selectivity >95%, which is comparable to the current industrial route (Figure 6b).[13] The above problems have been effectively solved by unique catalyst structure. With this catalyst, high oxime selectivity can also be achieved in a series of other ketones, indicating the generality of in-situ H_2O_2 generation for oxime synthesis. Apart from significant savings associated via in-situ-generated H_2O_2, if the lifetime of 0.33%Au-0.33%Pd/TS-1 catalyst was comparable to that of TS-1 reported in the current industrial route, it would result in a cost reduction of 13% (assuming a catalyst lifetime of 2.3 years). The environmental and economic savings from this development have shown us the potential of industrial organic conversions via in-situ-generated H_2O_2. Building on this, they discovered that introducing low concentrations of Pt into the AuPd nanoalloy can further enhance the catalytic performance due to the combined effect of continuous Pd clustering disruption and Pd oxidation state alteration.[58] In the oxidation of benzyl alcohol, Lyu et al. prepared a composite catalyst in which sub-nanometer Pd particles were encapsulated within the channels of hierarchically structured TS-1 (HTS-1).[59] Using the in-situ-generated H_2O_2 method, Pd@HTS-1 can achieve a benzyl alcohol oxidation rate of 4268.8 mmol h^{-1} kg_{cat}^{-1} with near 100% selectivity towards benzaldehyde. H_2O_2 molecules produced on Pd sites can overflow to the framework Ti^{4+} site to form Ti-OOH active species, selectively oxidizing chemisorbed benzyl alcohol to ben-

zaldehyde.

Although these reaction systems have addressed the issue of H_2O_2, the presence of H_2 poses inevitable safety concerns, and catalyst deactivation may occur quickly.[60] Ko et al. developed an integrated photoelectrochemical multiphase catalytic system that utilizes O_2 as the sole oxidant for the epoxidation of propylene, combining a nanostructured photocatalyst ($BiVO_4$ or TiO_2), an electro-catalyst consisting of atomically dispersed Co-N_x sites on carbon nanotubes (Co-N/CNT), with a multiphase catalyst based on TS-1.[61] The system allowed the in-situ generation of H_2O_2 from the photoelectrochemical ORR under light illumination, and enabled the direct epoxidation of propylene without H_2, sacrificial agents, or electrical energy. It enabled the stable production of propylene oxide (205 μmol within 24 hours) with a selectivity over 98% (Figures 6c and 6d). These studies have made significant advancements in the application of in-situ-generated H_2O_2 in organic conversion, but challenges remain in the long-term catalytic activity and scalability for industrial applications.[62]

Perspectives and outlook

Because the reactions involved are numerous and important, meanwhile new designs for producing H_2O_2 and organic reaction systems are increasingly approaching the needs of industrial applications, energy-saving green conversion with H_2O_2 has great application prospects. However, there are still some questions and expectations to be studied and realized. Herein, we have presented our perspectives on the future development of green organic conversions with H_2O_2:

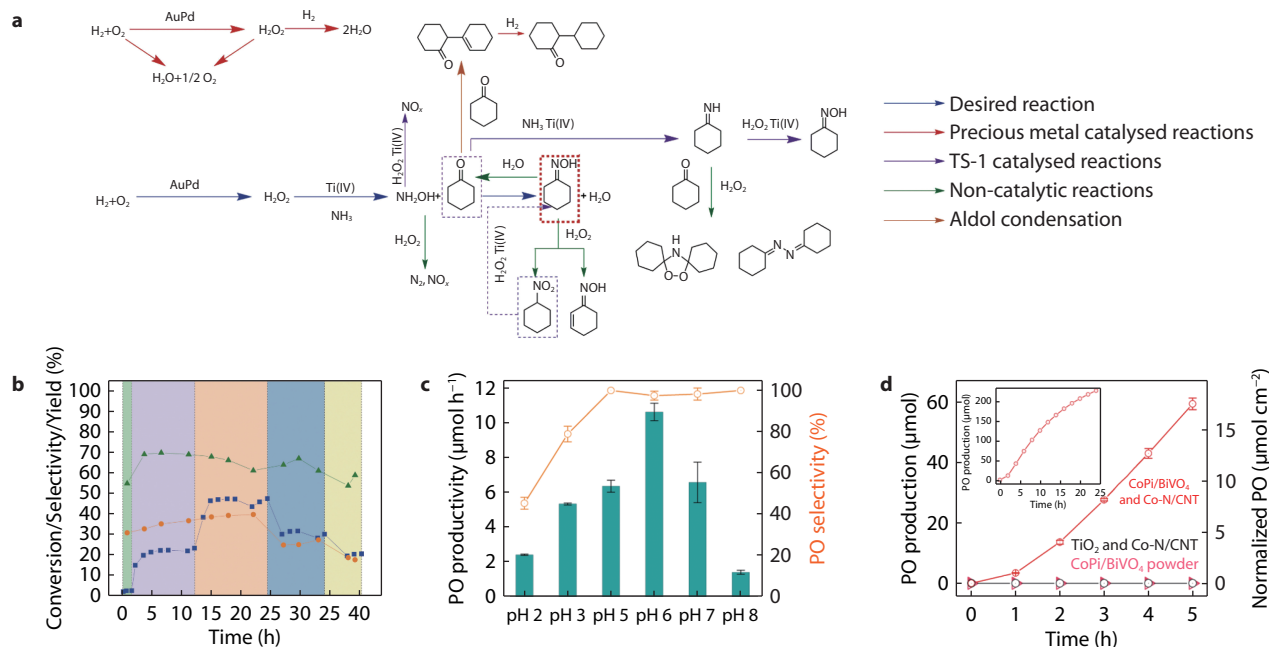(1) The activation pathway of H_2O_2 can directly affect the

Fig. 6 **a** Proposed reaction pathways in the ammoximation of cyclohexanone-to-cyclohexanone oxime via in-situ-generated H_2O_2. In-situ H_2O_2 was generated on AuPd nanoparticles by binding with commercial TS-1 catalyst. And direct synthesis of H_2O_2 is combined with cyclohexanone ammoximation to produce oxime yields comparable to commercial processes. **b** Optimization of reaction parameters for the 0.33%Au-0.33%Pd/TS-1(Acetate-O+R) catalyst in a continuous regime. Cyclohexanone oxime yield (blue squares), H_2 conversion (orange circles), H_2 selectivity (green triangles).[13] Copyright 2022, American Association for the Advancement of Science. **c** PO production rate and PO selectivity after 5 h of reaction in solutions with different pH values. **d** PO production in the presence of photo-electro-heterogeneous catalytic and photo-heterogeneous catalytic systems. Inset: PO production for 24 h.[61] Copyright 2021, Springer Nature.

efficiency and selectivity of organic reactions.[20–22] Because the activation of H_2O_2 may be influenced by multiple factors such as reaction microenvironment and catalyst structure, to date, we have not yet revealed the key factor that affects its activation pathway, making it difficult to achieve precise control over its activation pathway.[32, 36] In future research, emerging operando-detection techniques such as operando-SHINERS, operando-X-ray absorption spectroscopy (XAS), operando-transmission electron microscope (TEM), can be introduced to understand chemical bonds change, charge transfer behavior, and other important processes. In addition, the application of ultrafast spectroscopy techniques in this field may avoid the influence of external inputs on the catalyst structure or molecular chemical bonds in some in situ testing processes,[63] in order to obtain a more realistic reaction information.

(2) In electrochemical H_2O_2 production reactions, using some practical equipment such as: gas-diffusion electrodes and membrane electrode assemblies for electrochemical H_2O_2 production can provide data that better reflects industrial conditions. [64] In addition, electrochemical H_2O_2 production usually requires high concentrations of electrolyte, but separating H_2O_2 from the electrolyte is a huge challenge. Therefore, the development of electrolyte-free H_2O_2 production process is an important direction. In the production of high concentration H_2O_2, low selectivity and instability are often encountered.[39, 40] The competitive relationship between H_2O_2 production reaction and other reactions (OER and HER) may be effectively improved by regulating the composition and electronic structure of catalysts. On-demand production

of H_2O_2 and coupling of upstream and downstream reactions can alleviate the transport and decomposition problems.[65] In terms of this issue, the organic conversion reactions via electrochemical in-situ-generated H_2O_2 show significant potential.

(3) In photochemical and photoelectrochemical H_2O_2 production, bulk and surface charge recombination is the crucial factor for low reaction efficiency.[39] Due to the inherent properties, it is challenging for some metal oxide photocatalysts to achieve efficient charge transfer.[66] The study for novel photocatalyst materials with adjustable structures and broad spectral absorption, such as MOFs and COFs, may also be investigated.[47] In addition, although some oxygen species have been detected in the reaction, whether they truly participate in the reaction and their roles have not been clearly revealed, which limits our understanding of H_2O_2 formation. A combination of operando-spectroscopy, nuclear magnetic resonance and theoretical simulations etc. can be used to reveal the dynamic changes of reaction species and provide important guidance for catalyst design.

(4) In in-situ-generated H_2O_2 reaction system, the mismatch between H_2O_2 production rates and organic reaction rates may lead to waste of raw materials and reduction of reaction conversion efficiency.[57] Therefore, it is essential to optimize reaction parameters and optimal reaction conditions, and meanwhile find the correlation between them. Currently, whether catalysts can remain stable for thousands of hours to meet industrial demands remains a challenge.[62] Furthermore, safety issues from mixture of hydrogen and oxygen and engineering challenges posed by the production on a large

scale cannot be ignored, and it is necessary to focus on the reaction under conditions closer to industrial-scale reaction systems. This system often requires mild reaction conditions,[58, 59] and how to extend this system to other important organic reactions under non-mild conditions will be a topic in expanding this field.

■ CONFLICT OF INTEREST

The authors declare no conflict of interest.

■ ACKNOWLEDGEMENT

■ AUTHORS CONTRIBUTION

Zhaosheng Li and Xiaoming Xu contributed to the writing and editing of this manuscript. All other authors contributed to the discussion and reviewing/editing of the manuscript before submission.

■ REFERENCES

1. T. Punniyamurthy, S. Velusamy, J. Iqbal, *Chem. Rev.*, 2005, 105, 2329
2. J. Schranck, A. Tlili, M. Beller, *Angew. Chem. Int. Ed.*, 2013, 52, 7642
3. Y. Shi, Y. Xia, Wen Langyou, L. Gao, G. Xu, B. Zong, *Chem. Ind. Eng. Prog.*, 2021, 40, 2048
4. A. Aquino, O. Korup, R. Horn, *Ind. Eng. Chem. Res.*, 2023, 62, 3098
5. Y. Shi, Y. Xia, G. Xu, L. Wen, G. Gao, B. Zong, *Chinese J. Chem. Eng.*, 2022, 41, 145
6. A. A. Ingle, S. Z. Ansari, D. Z. Shende, K. L. Wasewar, A. B. Pandit, *Environ. Sci. Pollut. Res. Int.*, 2022, 29, 86468
7. C. P. Gordon, H. Engler, A. S. Tragl, M. Plodinec, T. Lunkenbein, A. Berkessel, J. H. Teles, A. N. Parvulescu, C. Coperet, *Nature*, 2020, 586, 708
8. R. Vithalani, D. S. Patel, C. K. Modi, V. Sharma, P. K. Jha, *Appl. Organomet. Chem.*, 2020, 34, e5500
9. X. Xu, Y. Zhang, Y. Chen, C. Liu, W. Wang, J. Wang, H. Huang, J. Feng, Z. Li, Z. Zou, *Proc. Natl. Acad. Sci.*, 2022, 119, e2205562119
10. S. C. Perry, D. Pangotra, L. Vieira, L. I. Csepei, V. Sieber, L. Wang, C. Ponce de León, F. C. Walsh, *Nat. Rev. Chem.*, 2019, 3, 442
11. C. Xia, J. Y. Kim, H. Wang, *Nat. Catal.*, 2020, 3, 605
12. C. M. Crombie, R. J. Lewis, R. L. Taylor, D. J. Morgan, T. E. Davies, A. Folli, D. M. Murphy, J. K. Edwards, J. Qi, H. Jiang, C. J. Kiely, X. Liu, M. S. Skjøth-Rasmussen, G. J. Hutchings, *ACS Catal.*, 2021, 11, 2701
13. R. J. Lewis, K. Ueura, X. Liu, Y. Fukuta, T. E. Davies, D. J. Morgan, L. W. Chen, J. Z. Qi, J. Singleton, J. K. Edwards, S. J. Freakley, C. J. Kiely, Y. Yamamoto, G. J. Hutchings, *Science*, 2022, 376, 615
14. M. Taramasso, G. Perego, B. Notari, U. S. Patent: 4, 410, 501[P], 1983.
15. X. Liang, Z. Mi, Y. Wang, L. Wang, X. Zhang, W. Wu, E. Min, S. Fu, *J. Chem. Technol. Biot.*, 2004, 79, 658
16. G. Blanco-Brieva, M. C. Capel-Sanchez, M. P. de Frutos, A. Padilla-Polo, J. M. Campos-Martin, J. L. G. Fierro, *Ind. Eng. Chem. Res.*, 2008, 47, 8011
17. T. Cousin, G. Chatel, N. Kardos, B. Andrioletti, M. Draye, *Catal. Sci. Technol.*, 2019, 9, 5256
18. K. Dong, Y. Wang, L. Zhang, X. Fan, Z. Li, D. Zhao, L. Yue, S. Sun, Y. Luo, Q. Liu, A. A. Alshehri, Q. Li, D. Ma, X. Sun, *Green Chem.*, 2022, 24, 8264
19. S. Tian, C. Peng, J. Dong, Q. Xu, Z. Chen, D. Zhai, Y. Wang, L. Gu, P. Hu, H. Duan, D. Wang, Y. Li, *ACS Catal.*, 2021, 11, 4946
20. X. Li, Q. Wang, J. Lyu, X. Li, *ChemistrySelect*, 2021, 6, 9735
21. Y. Wan, Q. Liang, Z. Li, S. Xu, X. Hu, Q. Liu, D. Lu, *J. Mol. Catal. A Chem.*, 2015, 402, 29
22. S. Ito, Y. Kon, T. Nakashima, D. Hong, H. Konno, D. Ino, K. Sato, *Molecules*, 2019, 24, 2520
23. C. Che, W. Yip, W. Yu, *Chem. Asian J.*, 2006, 1, 453
24. M. N. Timofeeva, O. A. Kholdeeva, S. H. Jhung, J. S. Chang, *Appl. Catal. A*, 2008, 345, 195
25. Y. Zhang, X. Dai, J. Wang, J. Liang, J. Rabeah, X. Tian, X. Yao, Y. Wang, S. Pang, *ChemSusChem*, 2023, 16, e202202104
26. Y. Zeng, T. Chen, X. Zhang, Y. Chen, H. Zhou, L. Yu, *Appl. Organomet. Chem.*, 2022, 36, e6658
27. L. Balapoor, R. Bikas, M. Dargahi, *Inorg. Chim. Acta*, 2020, 510, 119734
28. Y. Kon, T. Nakashima, A. Yada, T. Fujitani, S. Y. Onozawa, S. Kobayashi, K. Sato, *Org. Biomol. Chem.*, 2021, 19, 1115
29. J. Wang, H. Yu, Z. Wei, Q. Li, W. Xuan, Y. Wei, *Research*, 2020, 2020, 3875920
30. Y. Zhang, N. Zhang, T. Wang, H. Huang, Y. Chen, Z. Li, Z. Zou, *Appl. Catal. B*, 2019, 245, 410
31. N. V. Maksimchuk, V. Y. Evtushok, O. V. Zalomaeva, G. M. Maksimov, I. D. Ivanchikova, Y. A. Chesalov, I. V. Eltsov, P. A. Abramov, T. S. Glazneva, V. V. Yanshole, O. A. Kholdeeva, R. J. Errington, A. Solé-Daura, J. M. Poblet, J. J. Carbó, *ACS Catal.*, 2021, 11, 10589
32. N. V. Maksimchuk, I. D. Ivanchikova, G. M. Maksimov, I. V. Eltsov, V. Y. Evtushok, O. A. Kholdeeva, D. Lebbie, R. J. Errington, A. Solé-Daura, J. M. Poblet, J. J. Carbó, *ACS Catal.*, 2019, 9, 6262
33. J. Li, C. Xiao, K. Wang, Y. Li, G. Zhang, *Environ. Sci. Technol.*, 2019, 53, 11023
34. H. Zheng, Y. Zeng, J. Chen, R. Lin, W. Zhuang, R. Cao, Z. J. Lin, *Inorg. Chem.*, 2019, 58, 6983
35. C. Ling, X. Liu, H. Li, X. Wang, H. Gu, K. Wei, M. Li, Y. Shi, H. Ben, G. Zhan, C. Liang, W. Shen, Y. Li, J. Zhao, L. Zhang, *Angew. Chem. Int. Ed.*, 2022, 61, e202200670
36. Z. Yang, J. Qian, A. Yu, B. Pan, *Proc. Natl. Acad. Sci.*, 2019, 116, 6659
37. Q. Yan, C. Lian, K. Huang, L. Liang, H. Yu, P. Yin, J. Zhang, M. Xing, *Angew. Chem. Int. Ed.*, 2021, 60, 17155
38. Y. Xue, Y. Wang, Z. Pan, K. Sayama, *Angew. Chem. Int. Ed.*, 2021, 60, 10469
39. N. Karamoschos, D. Tasis, *Energies*, 2022, 15, 6202
40. H. Lu, X. Li, S. A. Monny, Z. Wang, L. Wang, *Chinese J. Catal.*, 2022, 43, 1204
41. X. Shi, S. Back, T. M. Gill, S. Siahrostami, X. Zheng, *Chem*, 2021, 7, 38
42. S. Li, J. Ma, F. Xu, L. Wei, D. He, *Chem. Eng. J.*, 2023, 452, 139371
43. E. Berl1, *Trans. Electrochem. Soc.*, 1939, 76, 359
44. C. Xia, Y. Xia, P. Zhu, L. Fan, H. Wang, *Science*, 2019, 366, 226
45. K. Wu, D. Wang, X. Lu, X. Zhang, Z. Xie, Y. Liu, B.-J. Su, J.-M. Chen, D.-S. Su, W. Qi, S. Guo, *Chem*, 2020, 6, 1443
46. Y. Wen, T. Zhang, J. Wang, Z. Pan, T. Wang, H. Yamashita, X. Qian, Y. Zhao, *Angew. Chem. Int. Ed.*, 2022, 61, e202205972
47. Y. Kondo, Y. Kuwahara, K. Mori, H. Yamashita, *Chem*, 2022, 8, 2924
48. Y. Zhang, C. Pan, G. Bian, J. Xu, Y. Dong, Y. Zhang, Y. Lou, W. Liu, Y. Zhu, *Nat. Energy*, 2023, 8, 361
49. H. Yang, C. Li, T. Liu, T. Fellowes, S. Y. Chong, L. Catalano, M. Bahri, W. Zhang, Y. Xu, L. Liu, W. Zhao, A. M. Gardner, R. Clowes, N. D. Browning, X. Li, A. J. Cowan, A. I. Cooper, *Nat. Nanotechnol.*, 2023, 18, 307
50. W. Zhang, P. Zhang, Q. Yang, K. Li, *Chinese J. Org. Chem.*, 2022, 42, 732

51. S. J. Freakley, S. Kochius, J. van Marwijk, C. Fenner, R. J. Lewis, K. Baldenius, S. S. Marais, D. J. Opperman, S. T. L. Harrison, M. Alcalde, M. S. Smit, G. J. Hutchings, *Nat. Commun.*, 2019, 10, 4178

52. Z. Jiang, L. Wang, J. Lei, Y. Liu, J. Zhang, *Appl. Catal. B*, 2019, 241, 367

53. F. Li, Q. Shao, M. Hu, Y. Chen, X. Huang, *ACS Catal.*, 2018, 8, 3418

54. A. Prieto, M. Palomino, U. Díaz, A. Corma, *Appl. Catal. A*, 2016, 523, 73

55. W. Lee, L. Lai, M. Cem Akatay, E. A. Stach, F. H. Ribeiro, W. N. Delgass, *J. Catal.*, 2012, 296, 31

56. N. Callaghan and J. A. Sullivan, *Appl. Catal. B*, 2014, 146, 258

57. R. J. Lewis, K. Ueura, X. Liu, Y. Fukuta, T. Qin, T. E. Davies, D. J. Morgan, A. Stenner, J. Singleton, J. K. Edwards, S. J. Freakley, C. J. Kiely, L. Chen, Y. Yamamoto, G. J. Hutchings, *ACS Catal.*, 2023, 13, 1934

58. R. J. Lewis, K. Ueura, Y. Fukuta, T. E. Davies, D. J. Morgan, C. B. Paris, J. Singleton, J. K. Edwards, S. J. Freakley, Y. Yamamoto, G. J. Hutchings, *Green Chem.*, 2022, 24, 9496

59. J. Lyu, J. Niu, F. Shen, J. Wei, Y. Xiang, Z. Yu, G. Zhang, C. Ding, Y. Huang, X. Li, *ACS Omega*, 2020, 5, 16865

60. A. K. Sinha, S. Seelan, S. Tsubota, M. Haruta, *Angew. Chem. Int. Ed.*, 2004, 43, 1546

61. M. Ko, Y. Kim, J. Woo, B. Lee, R. Mehrotra, P. Sharma, J. Kim, S. W. Hwang, H. Y. Jeong, H. Lim, S. H. Joo, J.-W. Jang, J. H. Kwak, *Nat. Catal.*, 2022, 5, 37

62. L. Lu, B. Fang, *Chem*, 2022, 8, 1548

63. A. Zong, B. R. Nebgen, S. Lin, J. A. Spies, M. Zuerch, *Nat. Rev. Mater.*, 2023, 8, 224

64. M. Dan, R. Zhong, S. Hu, H. Wu, Y. Zhou, Z. Liu, *Chem Catal.*, 2022, 2, 1919

65. S. Kala Thirumalaikumaran, R. Suwathy, M. Venkatesan, *J. Aerosp. Technol. Manag.*, 2018, 10, e2818

66. S. Corby, R. Rao, L. Steier, J. R. Durrant, *Nat. Rev. Mater.*, 2021, 6, 1136

67. M. Y. Qi, M. Conte, M. Anpo, Z. R. Tang, Y. J. Xu, *Chem. Rev.*, 2021, 121, 13051

68. Y. H. Li, Z. R. Tang, Y. J. Xu, *Chinese J. Catal.*, 2022, 43, 708

69. Y. L. Wu, M. Y. Qi, C. L. Tan, Z. R. Tang, Y. J. Xu, *Chinese J. Catal.*, 2022, 43, 1851

70. J. Y. Li, M. Y. Qi, Y. J. Xu, *Chinese J. Catal.*, 2022, 43, 1084

71. Z. Zhang, T. Tsuchimochi, T. Ina, Y. Kumabe, S. Muto, K. Ohara, H. Yamada, S. L. Ten-no, T. Tachikawa, *Nat. Commun.*, 2022, 13, 1499
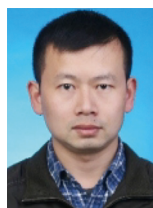
Biographies
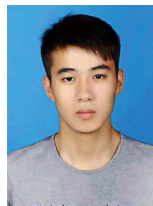
Xiaoming Xu obtained his bachelor's degree in Materials Science and Engineering from Zhengzhou University in 2019. Now, he is a Ph.D. student at Nanjing University under the supervision of Prof. Zhaosheng Li. His research interest mainly focuses on the study of H_2O_2 activation and utilization.

Zhaosheng Li received his Ph.D. degree in Condensed Matter Physics from the Institute of Solid State Physics, Chinese Academy of Sciences, in 2003. After a two-year postdoctoral fellowship at Nanjing University, he became a Lecturer at this university. In 2006, he was promoted to Associate Professor. Since 2011, he has become a full Professor of Materials Science and Engineering at the College of Engineering and Applied Sciences, Nanjing University. His current research interest includes photochemistry and photocatalysis.